IMPROVED CHARACTERIZATION OF UNCONVENTIONAL RESERVOIRS BY ANISOTROPY OF MAGNETIC SUSCEPTIBILITY

Norbert Schleifer[(1)], Nina Gegenhuber[(2)] and Robert Scholger[(2)]

(1) Wintershall Holding GmbH, Central Laboratory, Germany; (2) Montanuniversität Leoben, Chair of Applied Geophysics, Austria

This paper was prepared for presentation at the International Symposium of the Society of Core Analysts held in Vienna, Austria, 27 August – 1 September 2017

ABSTRACT

The re-evaluation of the legacy data of two Rotliegend gas-wells within the Northern German basin required a routine core analysis program which was designed including the non-destructive measurement of the anisotropy of the magnetic susceptibility (AMS).

The main objective of this approach was to see whether the depositional environment of the sedimentary rocks can be correlated with the degree of magnetic anisotropy. The study should further clarify whether adding rock magnetic properties to a core analysis program leads to an improved understanding of unconventional reservoir rock.

The program covered basic petrophysical parameters as porosity, gas-permeability and grain density, but also ultrasonic velocity (shear and compressional wave) and internal surface area (S_{por}). Magnetic Properties were measured at the Paleomagnetic Laboratory of the MU Leoben. Advanced magnetic methods were included to identify the iron minerals dominating the magnetic properties and the orientation of its remanent (permanent) magnetization. Results show that environments which represent low energetic deposits can be identified by low porosities and permeabilities, but also by a high magnetic susceptibility and an anisotropy characterized by a shape parameter ranging from positive to negative values. On the other hand, higher energetic depositional environments as dunes and sandflats are characterized by high porosities and permeabilities as well as low magnetic susceptibility and a positive shape parameter.

In contrast to the other petrophysical parameters the AMS shape parameter of distinct facies show differences between investigated wells and within single members of the Rotliegend Waste Zone. The abundance and orientation of minerals with higher magnetic susceptibility, e.g. iron minerals, clays, is obviously correlated to certain depositional environments and has also an impact on the key petrophysical parameters porosity and permeability.

INTRODUCTION

Around 2010 it was decided to re-evaluate the tight gas-potential of the sandstones of the so-called “Rotliegend waste zone” in the Northern German Basin. The Rotliegend is of

Permian age. The "Waste Zone" is defined by five members of the Hannover formation below the Zechstein formation and above the conventionally produced Wustrow Member. Samples for this study come from the Bahnsen, Niendorf and Munster members. Thickness of the "Waste Zone" can reach up to 125 m as in the fairway north of Hannover. The RWZ consists of Sabkha sediments (Neuendorf et al., 2005) deposited in the vicinity of a salt lake dominated by silts and clays with sands associated mainly with thick silt deposits. As the size of the salt lake varied throughout time depositional environments with different energetic levels are present. Samples from two wells RWZ 1(B) and RWZ 2(D) were investigated for this study covering a variety of depositional environments. These facies and their characteristics are listed in Table 1. Core description and facies definition along the cores is based on gamma-ray well log cut-offs. Some zones remain "undefined" in terms of facies category.

ROUTINE CORE ANALYSIS PROGRAM

After reviewing the available legacy data it became clear that laboratory techniques in the 1970's were limited to permeability measurements above 0.1 mD. The new measurements covered 58 plugs from well RWZ 1(B) and 131 plugs from well RWZ 2(D). Plug diameter and height is 30 mm.
Precipitated salt while storage was removed by immersion in 2%-KCl brine. Conductivity of the brine was monitored until no further increase was observed.
The program covered the following measurements.

- Steady state air-permeability
- Porosity and grain density using Archimedes principle
- Specific pore surface area S_{por} by N_2-adsorption using BET method
- Ultrasonic velocity of compressional V_p and shear waves V_s

Experiments

Steady State Air-Permeability

Air-permeability is measured by a steady-state setup using atmospheric flow mode. Confining pressure is set to 400 psi. Each measurement was repeated three times. Klinkenberg permeability is calculated based on the equation by Riekmann, 1970,

$K_a = K_L/(1+0.5*K_L^{-0.37}/P_m)$
with

K_a: apparent permeability, K_L: Klinkenberg permeability, P_m: mean pressure

Porosity and Grain Density

Archimedes principle using isopropyl-alcohol was applied to measure porosity and permeability. Cleaned samples were dried at 80°C and weighted. 100% saturation was achieved by immersion of the samples under vacuum pressure. Samples stayed immersed till the weighting cycle was finished.

Specific Pore Surface area (S_{por})

The measurement of S_{por} was run on 30 selected samples at the Chair of Mineral Processing at MUL. A Test requires 10g of sample material. Samples were heated at 200 °C up to 4 hours to establish constant dry weight. Weight changes were monitored. A Flowsorb 2300© Micromeritics™ instrument was used. Surface area in units m^2/g was determined by nitrogen adsorption as well as desorption using BET method.

Ultrasonic velocity of compressional V_p and shear waves V_s

Ultrasonic velocities were determined at ambient conditions without confining stress on dry samples. Compressional (V_p) and shear wave (V_s) velocity probes were used with a frequency of 1 MHz (Gegenhuber & Schön, 2014). Wave propagation was along the cylindrical axis of the plugs.

ANISOTROPY OF MAGNETIC SUSCEPTIBILITY (AMS)

Magnetic susceptibility k_m describes the behaviour of a material in a magnetic field (Thompson & Oldfield, 1986) and is a non-destructive method. Sediments and sedimentary rocks show low magnetic susceptibilities compared to other rock types like volcanic or metamorphic rocks. Abundant minerals as quartz, calcite and kaolinite show diamagnetic behavior resulting in negative values. Abundance of paramagnetic minerals in contrast increase k_m, e.g. illite, micas and siderite, chlorite. Examples for the application of the method in core analysis are given by Potter, 2007 and Potter et al., 2011. As other petrophysical parameters like permeability and ultrasonic velocity, K_m is a directional dependent parameter. During sedimentation magnetic minerals can be aligned along a preferential direction or within a plane. This process is influenced by particle size and shape, dynamics of the depositional environment, direction of the current magnetic field and post-sedimentary processes. The resulting anisotropy of magnetic susceptibility (AMS) is characterized by an ellipsoid, whose axes are defined by maximum susceptibility (k_{max}), intermediate susceptibility (k_{int}) and minimum susceptibility (k_{min}). Several parameters are defined to the shape and degree of anisotropy (Table 3). The main anisotropy parameter referred to in this paper, is shape parameter T. In general a positive T close to 1 characterizes an oblate shaped ellipsoid. Low energetic environments or depositional environments without predominant flow direction should show this AMS behaviour. Deposits with a dominant flow direction within a bedding plane also result in a flat ellipsoid but the dominant flow direction should be represented by a $k_{max} > k_{int}$ within the bedding plane if the remanence carriers are dominantly multidomain magnetite (Potter

& Stephenson, 1988). This results in a lower positive shape parameter T. Negative T values are assigned to prolate shaped ellipsoid. This means that there is a dominant flow direction but no alignment within a bedding plane ($k_{max} > k_{int}$, $k_{int} \sim k_{min}$). Shape parameters close to zero represent no pronounced AMS with a $k_{max} \sim k_{int} \sim k_{min}$. All measurements were carried out with a AGICO MFK 1 Multifunctional Kappabridge.

NATURAL REMANENT MAGNETIZATION

The natural remanent magnetization (NRM) (Thompson&Oldfield, 1986) is defined as the magnetization of a rock which is also present without an external magnetic field. Titanium-iron oxides are the main carriers of this magnetization. There are several processes whereby an NRM can be created, e.g. cooling of rocks below the Curie-temperature (thermoremanent magnetization) in the Earth's magnetic field leads to the alignment of mineral domains and the resulting NRM records the prevailing Earth's magnetic field direction (assuming the sample is not very anisotropic).

In the Paleomagnetic laboratory of MUL the paleomagnetic field is investigated by a 2G Cryogenic Magnetometer Modell 760-4K. Carriers of NRM can be investigated by stepwise destroying the NRM by heating up to the Curie temperature or by applying strong alternating magnetic fields (AF). Achieving a saturated isothermal remanent magnetization (SIRM) aligning all the magnetic domains along a strong applied field also gives insight into the abundant iron minerals. The ratio of remanent magnetization to induced magnetization is called the Remanence-factor or Königsberger Factor Q. The induced magnetization is calculated multiplying K_m with the average Earth's magnetic field strength (50 µT).

RESULTS

The distribution of the depositional environments within the porosity-permeability cross-plot are shown in Figure 1. A maximum porosity of 19.3 % and a maximum permeability of 140.5 mD are found in well RWZ1 (B). Most of the samples from well RWZ2 (D) lie below 10% porosity and have a Klinkenberg permeability K_L between 0.001 to 10 mD. Samples from low energetic depositional environments like pond/lake, aeolian mudflat and low energetic fluvial deposit tend to have lower porosities and permeabilities. The sandflat deposits cannot be discriminated and show a distribution above 1% porosity and between 0.01 and 100 mD. Aeolian dune (base) show intermediate values.

Looking at the susceptibility (K_m) and shape parameter (T) cross-plots, depositional environments can be distinguished (Fig. 2). In well RWZ 1(B) high susceptibility ($100*10^{-6}$ SI $< K_m <$ $1000*10^{-6}$ SI) is associated to samples from low energetic fluvial deposits, pond/lake and aeolian mudflat. Shape parameters of this samples vary between positive and negative values. Aeolian dune (base), dry, damp and wet sandflat samples have low to intermediate K_m but are characterized by T values mainly above 0.5. In well RWZ 2 (D) no clear discrimination of the depositional environment is possible based solely on K_m. However again dry, damp and wet sandflat samples are associated to high T values. In contrast to well RWZ 1 (B) pond/lake samples have only positive T values and aeolian dune (base) samples show T values around zero. Samples from low energetic fluvial

deposits can be found with positive as well as negative T values, with the majority in the positive range.
Comparing the magnetic carriers within each well and facies (Table 3) one can see that despite aeolian mudflat, pond/lake and low energetic fluvial deposit samples in well RWZ 1(B) magnetite is the dominant iron mineral and in well RWZ 2(D) hematite is the dominant iron mineral. Correlations with other petrophysical parameters as compressional wave velocity V_p and specific surface area S_{por} measured via nitrogen adsorption are shown in Figure 3. High velocities and susceptibilities are associated with aeolian mudflat, pond/lake and low energetic fluvial deposits. Velocities below 4000 m/s and susceptibilities below $250*10^{-6}$ SI are associated with sandflat deposits as well as aeolian dune (base). Adsorption S_{por} versus K_m show a different distribution. Aeolian mudflat,pond/lake and low energetic fluvial deposit have highest values ($S_{por} > 1$ m^2/g; $K_m > 100*10^{-6}$ SI). Dry and amp sandflat together with aeolian dune (base) show lowest values (S_{por} a 0.1-1 m^2/g; $K_m < 100*10^{-6}$ SI).
Wet sandflat samples are in the same S_{por} range but show Km values above $100*10^{-6}$ SI.
Compiling the results of petrophysical measurements facies dependent parameters can be found. An example is given in Table 4. Within Niendorf member of well RWZ2 (D) correlations could be found allowing to distinguish between the four depositional environments: Aeolian mudflat, dry, damp and wet sandflats. Parameters leading to this discrimination are K_m, NRM, Shape parameter T, porosity and permeability. Figure 4 shows a depth plot of these parameters within the Niendorf member of RWZ2 (D).

DISCUSSION

The conventional porosity-permeability cross-plots show the expected distribution with clay rich facies as pond/lake and aeolian mudflat having lowest values (Fig.1). Facies with no or less clay, as aeolian dune (base) and dry sandflat show highest porosity and permeability. As their clay content lie in a narrow range the damp and wet sandflat as well as the low energetic fluvial deposits show a wider range of permeability even higher than the dry sandflat facies. S_{por} is a parameter which is dominated by clay content. In Figure 3 the sandflat facies have overlapping S_{por} which explains the wide variation of permeability within these facies. Aeolian dune (base) show a tendency towards higher S_{por} which might be explained by a higher fraction of finer sand grains. Although the fluvial deposits are distributed in the lower permeability range their S_{por} is comparable with sandflats and aeolian dune (base). The impact of grain size and grain contacts is measured by compressional wave velocity V_p (Fig. 3). Aeolian dune (base) and sandflats show lowest velocities based on larger grain sizes and higher porosities compared to clay rich facies. Magnetic susceptibility supports this discrimination. In well RWZ 1(B) pond/lake, aeolian mudflat and low energetic fluvial deposits are characterized by high susceptibility and shape parameters varying between -0.5 and 1 (Fig. 2, left). Fluvial deposits in well RWZ 2(D) show a different behavior. They have a lower K_m but a tendency towards positive T values (Fig. 2, right). Permeability and porosity values of this facies are also higher in well RWZ 2(D). Although less abundant, a better alignment of hematite, as magnetic carrier (Table 3) seems to exist in this well.

The AMS of the investigated environmental deposits shows differences between the two wells which do not become obvious when looking at the conventional porosity-permeability correlation. Aeolian dune (base) samples show distinct positive T values in well RWZ 1(B) but values close to zero in well RWZ 2 (D). The same shift towards lower values can be observed within the sandflat and aeolian mudflat facies. In contrast pond/lake and low energetic fluvial deposit samples show a trend towards more positive T values. The impact of magnetic carriers and their domain state on AMS in this study has not been fully understood yet (Potter & Stephenson, 1988), however the different distributions of the shape parameters within the two wells might be an indication for that.
Acidization or mobilization of iron minerals (Gaupp&Schöner, 2008) might be another reason for weaker foliation in the lower energetic deposits than in the higher energetic deposits. A magnetic overprint by the coring process could be identified in both wells with a stronger impact on samples of well RWZ 2(D). The example of well RWZ 2(D), Niendorf member (Table 4, Fig. 4) shows that depositional environments are distinguishable by using a compilation of the petrophysical parameters K_m, NRM, T, porosity and permeability. The facies aeolian mudflat and damp sandflat also show that their shape parameter can change from positive to negative values within a Rotliegend member of a single well.

CONCLUSIONS

The study shows that implementation of AMS leads to an improved petrophysical discrimination of depositional environments compared to conventional porosity-permeability cross-plots. All samples included in the study show a measurable and distinct anisotropy. As the method is cheap and non-destructive it can be easily included in conventional core analysis workflows. Interpretation of the results however need additional rock magnetic studies to identify the magnetic carriers and to understand post-sedimentary impacts on magnetic anisotropy. AMS response of depositional environments and main magnetic carrier change between two wells of same stratigraphy. Even within a single well and within a single Rotliegend member same depositional environments defined by core description appear different in their AMS response.

NOMENCLATURE

AF: Alternating magnetic field.
AMS: Anisotropy of magnetic susceptibility
BET: Interpretation of nitrogen adsorption/desorption data (Brunauer et al., 1938).
K_a: apparent (measured) permeability
K_L: Klinkenberg corrected permeability.
K_m: (Mean) magnetic suceptibility.
K_{max}, K_{int}, K_{min}: maximum, intermediate and minimum susceptibility.
NRM: Natural remanent magnetization
P_m: Mean Pressure
Q: Remanence Factor, Königsberger Factor.
SIRM: saturated remanent magnetization.
Spor: Specific surface area in m^2/g measured by nitrogen adsorption.
V_p, V_s: Ultrasonic compressional and shear wave velocities (m/s).

ACKNOWLEDGEMENT

We would like to thank Wintershall Holding GmbH for the opportunity to present these results and for funding this study. Many thanks to all the colleagues involved and supporting the project.

REFERENCES

1. *Brunauer, S.; Emmett, P. H.; Teller, E. (1938):* Adsorption of Gases in Multimolecular Layers. Journal of the American Chemical Society. Vol. 60, No. 2, pp. 309–319.
2. *Gaupp, R. & Schöner, R. (2008):* Intra-reservoir generation of organic acids and late stage enhanced porosity in sandstone. AAPG Annual Conference. Article #40373.
3. *Gegenhuber, N. & Schön, J. (2014):* Thermal Conductivity Estimation from Elastic-Wave Velocity—Application of a Petrographic-Coded Model. Petrophysics, Vol. 55, No. 1, pp. 51–56.
4. *Neuendorf, K.; Mehl, J. and Jackson, J. (2005):* Glossary of Geology 5th edition. American Geological Institute.
5. *Potter, D. K. and Stephenson, A. (1988):* Single domain particles in rocks and magnetic fabric analysis. Geophysical Research Letters, 15, 1097-1100.
6. *Potter, D. K. (2007):* Magnetic susceptibility as a rapid, non-destructive technique for improved petrophysical parameter prediction. Petrophysics, Vol. **48**, No. 3), pp. 191-201.
7. *Potter, D. K., Ali, A., Imhmed, S. and Schleifer, N. (2011)*. Quantifying the effects of core cleaning, core flooding and fines migration using sensitive magnetic techniques: implications for permeability determination and formation damage. Petrophysics, Vol. **52**, No. 6, pp. 444-451.
8. *Riekmann, M. (1970):* Untersuchung von Turbulenzerscheinungen beim Fließen von Gasen durch Speichergesteine unter Berücksichtigung der Gleitströmung. Erdöl-Erdgas-Zeitschrift, Jg. 86, pp. 36-51.
9. *Thompson R. and Oldfield, F. (1986):* Environmental Magnetism: London, Allen & Unwin, 277 p.

Table 1: Depositional environments (facies) investigated in the study.	
Facies:	Classification
Aeolian dune (base)	Well bedded, fine to coarse sand deposits with upward increasing dip angles. Bases consist of sandstones with angels of 5-15° increasing upward to more than 15°. cross-bedding. Variation of sediments depend on wind velocity.
Aeolian mudflat	Wavy laminated claystones with lenses of siltstone, clay content > 50%, periodical subaerial deposition, sand and silt were blown into the clay deposit
Damp sandflat	Aeolian sands temporarily deposited under aquatic conditions, adhesive bound clay possible, clay content < 20%
Dry sandflat	No clay, maximum dip angle 5%
Wet sandflat	Aeolian sands deposited under wet conditions, clay/silt content 20 to 50%, clasts of clay deposited by high energetic flow.
Low energetic fluvial deposit	Low energetic, shallow braided stream channel system and sheetflood sediments. Fine grained to coarser sediments.
Pond/lake	Silt with high clay content (>95%), sand inclusions, lamination, low energetic deposit

Table 2: Definition of anisotropy parameters used in the study.				
Parameter	Equation	Oblate (disc)	Prolate (cigar)	Neutral
Mean susceptibility	$K_m=(k_{max}+k_{int}+k_{min})/3$	$k_{max} \sim k_{int} > k_{min}$	$k_{max} > k_{int} \sim k_{min}$	$K_{int}=(k_{min} * k_{max})/2$
Foliation F	$F = k_{int}/k_{min}$	high	low	F=L
Lineation L	$L = k_{max}/k_{int}$	low	high	L=F
Shape Parameter T	$T = (\ln(L) - \ln(F))/(\ln(L) + \ln(F))$	$0<T\leq1$	$-1\leq T<0$	T=0

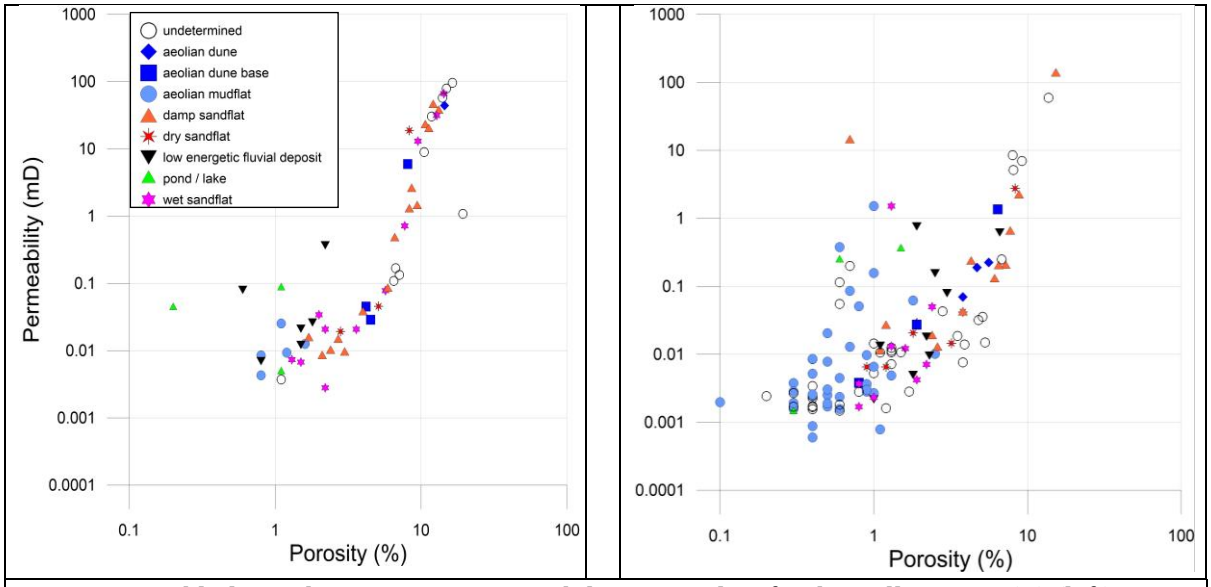

Figure 1: Double-logarithmic porosity-permeability cross-plots for the wells RWZ 1(B) (left); RWZ 2(D) (right) with indication of depositional environment.

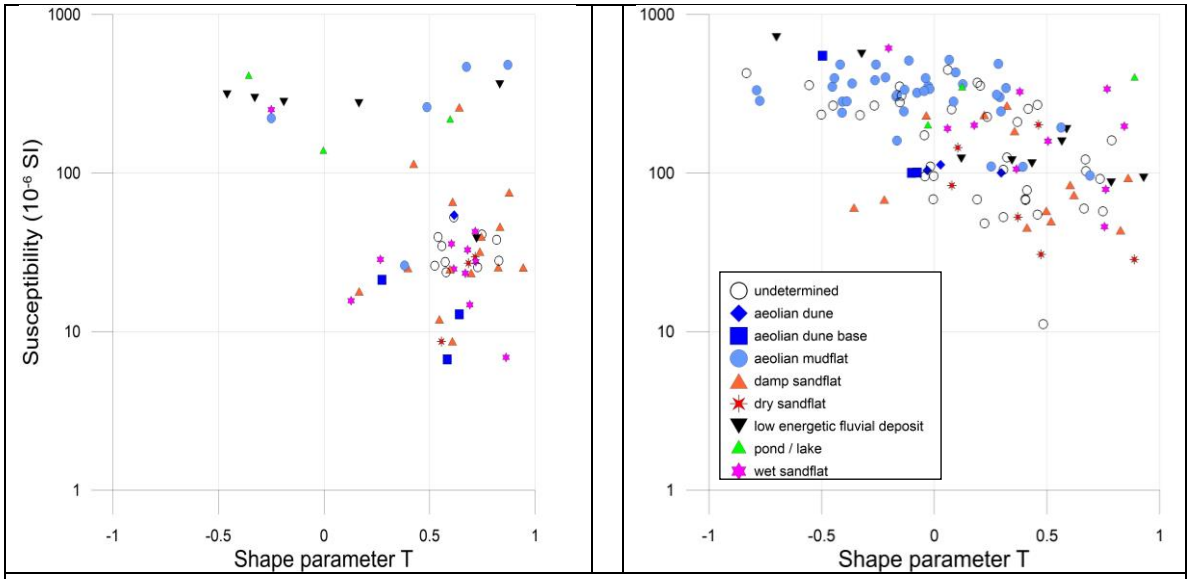

Figure 2: Shape Parameter T versus K_m for the wells RWZ 1(B) (left); RWZ 2 (D) (right) with indication of depositional environment.

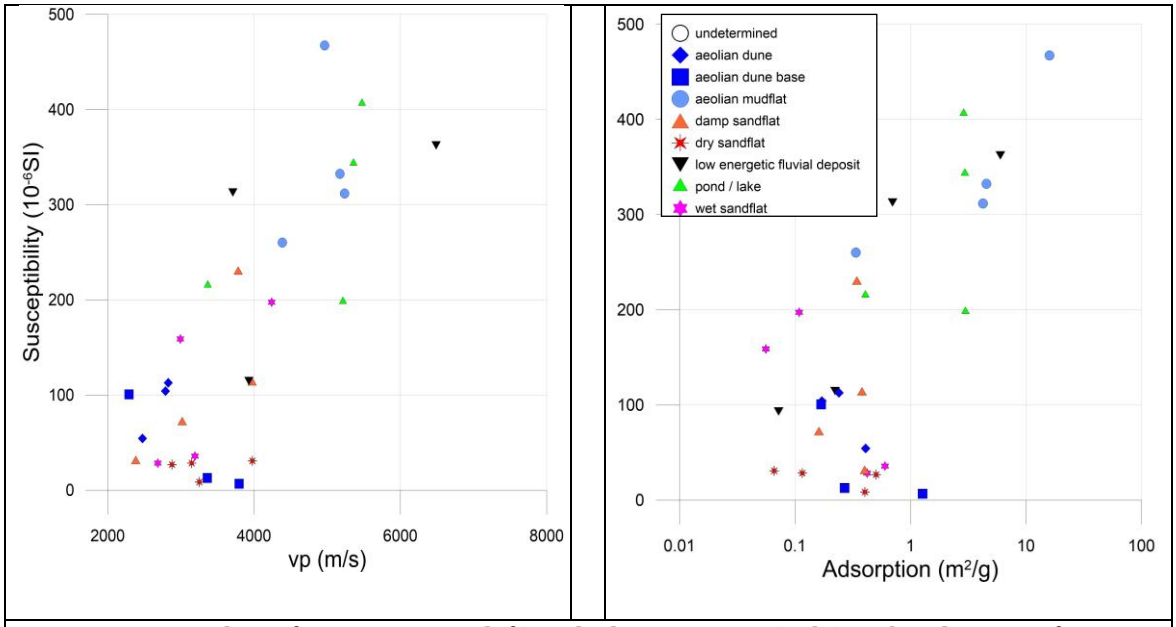

Figure 3: Cross-plots of K_m versus Vp (left) and adsorption S_{por} (right) with indication of depositional environment.

Table 3: Carriers of NRM within the depositional environments:		
Facies	**Well RWZ1 (B)**	**Well RWZ2 (D)**
Aeolian dune (base)	Magnetite	Hematite
Aeolian mudflat	Magnetite, hematite	Hematite
Wet sandflat	Magnetite	Hematite
Damp sandflat	Magnetite	Hematite
Dry sandflat	Magnetite	Magnetite
Low energetic fluvial deposit	Hematite	Hematite
Pond/lake	Hematite	Hematite

Table 4: Facies dependent petrophysical parameters within well RWZ2 (D) Niendorf member.			
Aeolian mudflat	***Dry sandflat***	***Damp sandflat***	***Wet sandflat***
high K_m	low to intermediate K_m	low Km	low Km
high NRM	low to intermediate NRM	low NRM	low NRM
-0.5< T < 0.75	T > 0	-0.5 < T < 1	T > 0
low porosity	high porosity	intermediate to high porosity	low porosity
low permeability	high permeability	intermediate to high permeability	low permeability

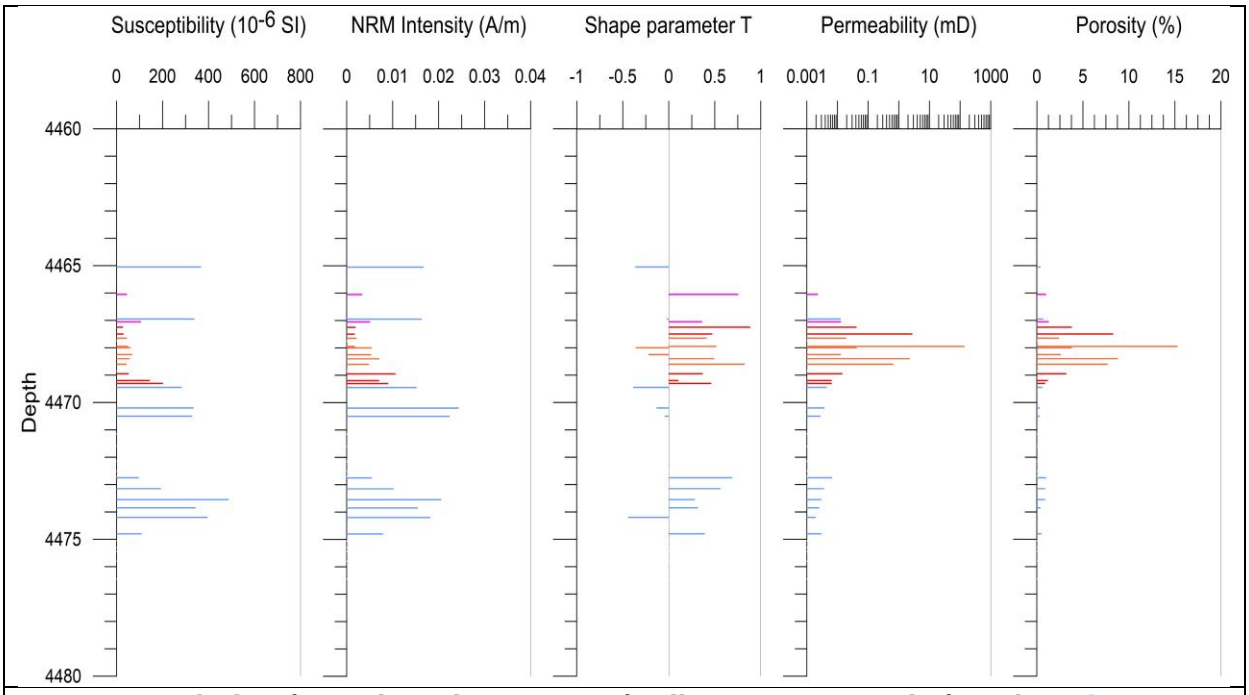

Figure 4: Depth plot of petrophysical parameters of well RWZ 2 (D), Niendorf member. Blue: Aeolian mudflat; Red: Dry sandflat; Orange: Damp Sandflat; Pink: Wet Sandflat (see also Table 4).